

# Estimation of Finger Joint Angles Based on Electromechanical Sensing of Wrist Shape

Junki Kawaguchi, Shunsuke Yoshimoto, *Member, IEEE*, Yoshihiro Kuroda, *Member, IEEE*, and Osamu Oshiro, *Member, IEEE*

**Abstract**—An approach to finger motion capture that places fewer restrictions on the usage environment and actions of the user is an important research topic in biomechanics and human-computer interaction. We proposed a system that electrically detects finger motion from the associated deformation of the wrist and estimates the finger joint angles using multiple regression models. A wrist-mounted sensing device with 16 electrodes detects deformation of the wrist from changes in electrical contact resistance at the skin. In this study, we experimentally investigated the accuracy of finger joint angle estimation, the adequacy of two multiple regression models, and the resolution of the estimation of total finger joint angles. In experiments, both the finger joint angles and the system output voltage were recorded as subjects performed flexion/extension of the fingers. These data were used for calibration using the least-squares method. The system was found to be capable of estimating the total finger joint angle with a root-mean-square error of 29–34 degrees. A multiple regression model with a second-order polynomial basis function was shown to be suitable for the estimation of all total finger joint angles, but not those of the thumb.

**Index Terms**—Electrical contact resistance, finger motion capture, multiple regression model, wrist shape deformation.

## I. INTRODUCTION

HUMAN motion capture is a major topic in research on biomechanics and human-computer interactions. The motion of different parts of the human body is used in a variety of areas [1], [2]. For example, in sports activities, hand and foot motions are used to analyze the throwing of an object or running to examine the mechanisms and dynamic characteristics of the human body. The use of human motion has also attracted considerable attention as a system input for the realization of ubiquitous interfaces. Because of its frequent use, the hand is an important target in human motion capture. Finger motion capture is useful in a variety of applications such as hand gesture recognition, control of electronics, sports training, musical instrument training, and rehabilitation and assistive technologies. This makes finger motion capture, and especially the measurement of finger joint angles, an important research topic. However, finger motion capture is challenging

Manuscript received April 12, 2016; revised September 1, 2016; accepted October 24, 2016. Date of publication November 9, 2016; date of current version September 2, 2017. This study was partially supported by the Japan Society for the Promotion of Science KAKENHI Grant Numbers JP25870394 and JP16H05875.

The authors are with the Graduate School of Engineering Science, Osaka University, Osaka 560-8531, Japan (e-mail: kawaguchi@bpe.es.osaka-u.ac.jp; yoshimoto@bpe.es.osaka-u.ac.jp; ykuroda@bpe.es.osaka-u.ac.jp; oshiro@bpe.es.osaka-u.ac.jp).

Digital Object Identifier 10.1109/TNSRE.2016.2626800

because of the complexity of the structure and motion of the human hand.

Optical tracking using a camera is a widely used approach to finger motion capture [3]–[6]. This method can capture finger motion without imposing any restrictions on the user's hand. However, it has drawbacks such as workspace limitations and occlusion. An alternative approach uses mechanical methods, in which a glove-type sensing device comprising a bending sensor, magnetic sensor, and accelerometer is used to measure the finger joint angles and hand position [7]–[10]. The mechanical method can capture finger motion accurately because the sensing device is directly mounted on the user's hand. However, such a device can disturb the natural finger motion and impede the delicate sense of touch. Indirect measurement has also been used to measure actions in a range of environments. Electromyography (EMG)-based methods, in which finger motion is tracked indirectly, offer an approach that potentially avoids the restrictions of the other methods [11]–[13], allowing several types of hand posture to be recognized using a simple sensing device to generate the system input [14]. However, EMG signals from several forearm muscles are required to track the finger joint angles. This means that there is a trade-off between the accuracy of measurement and the size of the sensing device.

To overcome these limitations, several approaches have focused on the musculoskeletal structure of the human body, using the activity of body parts other than the hand to track finger motion. For example, some methods estimate finger motion from deformations in the wrist shape when a finger moves. Fukui et al. proposed a method that used infrared photo reflectors to measure the wrist shape and estimate finger motion [15], [16]. This infrared-based method could recognize several types of hand posture from the measured wrist shape. However, ambient light may degrade the measurements. Rekimoto proposed a capacitance-based method, GestureWrist, which used the capacitance between the wrist-mounted sensing device and the user's wrist skin to recognize the hand posture [17]. As the measurements are made electrically, this method requires only a small device that is not influenced by environmental light. Dementev and Paradiso proposed a pressure-based method, WristFlex, in which the pressure applied by the wrist is measured by a mounted sensing device and used to recognize the hand posture [18]. This method limits the user's action to some extent owing to the need for compression of the wrist. Although these three methods have great benefits for unobtrusive gesture recognition, the estimation of finger joint angles has not yet been achieved.

Other methods have used the sounds generated by hand action, carried to the sensing device via bone conduction [19], [20]. Although these methods can distinguish different types of finger motion, their performance is significantly influenced by noise from the surrounding environment and from other body parts. Sikder et al. proposed an ultrasound-based method that was able to measure muscle activity through a wearable probe [21]. This method estimates the finger joint angles by analyzing muscle activity. However, it is influenced by a user's actions because the probe must be fixed firmly to the user's wrist. Lin et al. measured the skin strain on both back of the hand and the wrist to determine the hand posture [22]. Their method can accurately recognize the hand posture, because the back of the hand is close to the fingers and the movements of muscles and tendons can be observed relatively accurately. However, this method has been unable to determine the finger joint angles. To develop a finger motion capture method with fewer restrictions, we focused on the interlocked musculoskeletal structure, and investigated a novel electrical method for detecting deformation of the wrist shape, with the goal of estimating finger motion.

The novel electromechanical method proposed in this study capitalizes on the flexibility and conductivity of human skin. The deformation of the wrist shape is detected from the variation in electrical contact resistance in the contact area between the skin and electrodes. The system outputs a voltage corresponding to the electrical contact resistance, and the total finger joint angles are then estimated from the system output using multiple regression models. Because sensing is performed at the wrist, the finger motion can be estimated while imposing only small restrictions on the user's environment and actions. As the proposed method uses electrical sensing with a small and lightweight device mounted on the wrist, stable measurements can be made while placing a small burden on the user. In this paper, we investigated effective multiple regression model and tested the performance of the proposed method.

## II. METHODS

Because the musculoskeletal structure is interlocked, deformations in the wrist shape correspond to finger motions. Our proposed method detects these deformations from variations in the electrical contact resistance between the skin of the wrist and electrodes. A system overview is shown in Fig. 1. The user mounts a sensing device with multiple electrodes on his/her wrist. The circuit outputs a voltage corresponding to the finger motion, based on the following relationships:

- 1) The relationship between finger motion and deformation of the wrist shape. The human anatomy converts finger motion to deformation of the wrist.
- 2) The relationship between deformation of the wrist shape and variation in the contact area between the skin and electrodes. Deformation of the wrist causes variations within the contact area.
- 3) The relationship between variation in the contact area and electrical contact resistance. The sensing device detects a variation corresponding to deformation of the wrist as a variation in electrical contact resistance.

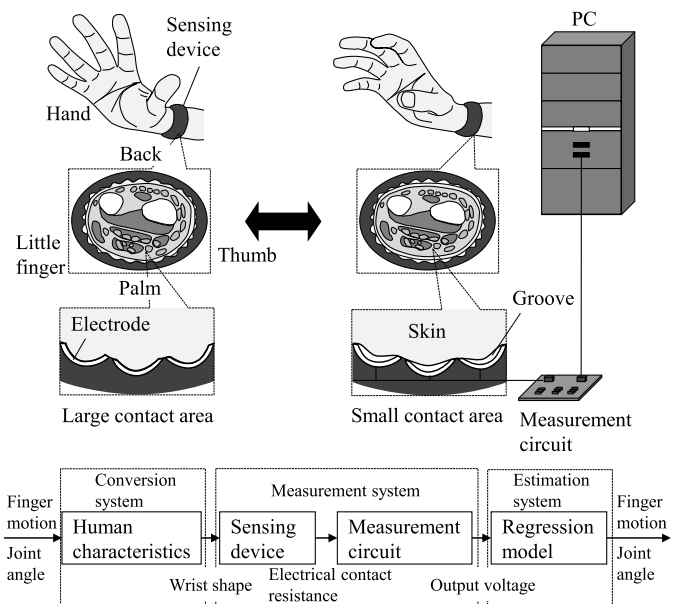


**Fig. 1.** System overview. The sensing device is mounted on the wrist and the measurement circuit outputs a voltage corresponding to the finger motion. The output voltage is recorded using a personal computer. The recorded voltage is used to estimate the finger joint angles.

- 4) The relationship between variation in electrical contact resistance and system output voltage. The measurement circuit outputs a voltage corresponding to the electrical contact resistance.

Each finger joint angle is estimated from the system output using a multiple regression model. The parameters of the multiple regression model that represent the relationship between the system output voltage and the finger joint angles were calculated in advance using the least-squares method (LSM). In this section, we describe the characteristics of the hand, the sensing device, the measurement circuit of the system, the multiple regression models, and the calibration process.

### A. Hand Characteristics

A human hand, which consists of 27 bones and 38 muscles, has 21 degrees of freedom of motion [23]. In this system, we discuss the 14 degrees of freedom of finger motion that are required for the flexion/extension of a finger. These are the angles of the interphalangeal (IP) and metacarpophalangeal (MP) joints of the thumb, and of the proximal interphalangeal (PIP), metacarpophalangeal (MP), and distal interphalangeal (DIP) joints of the other fingers. The muscles and tendons that are involved in the finger motion are located mainly at the wrist. When a finger is moved, the wrist shape is therefore deformed by the activity of these muscles and tendons. For example, when the index finger flexes from the posture of extending all fingers, the contraction of the flexor digitorum profundus muscle causes a part of the palm side of the wrist to become hollow. Because the muscles and tendons corresponding to each finger motion are distributed across the wrist, the state of deformation of the wrist shape is different for each motion of each finger. We therefore assumed that it would be possible to estimate finger motion with a given degree of freedom from the motion of the wrist.

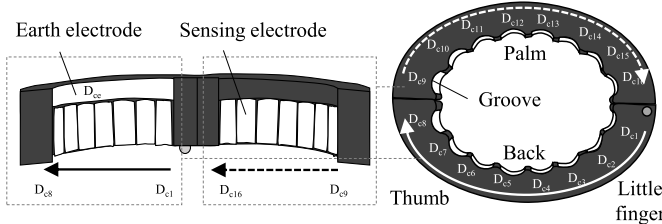


**Fig. 2.** Sensing device. The sensing device has multiple grooves, with sensing electrodes  $D_{ci}$  ( $i = 1, 2, \dots, 16$ ) arranged on them. An earth electrode  $D_{ce}$  is also attached to the sensing device.

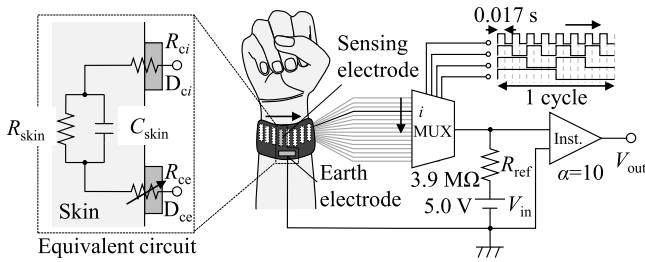


**Fig. 3.** Measurement circuit. Multiple sensing electrodes are switched using a multiplexer. The circuit outputs a voltage corresponding to the electrical contact resistance of each sensing electrode.

### B. Measurement System

The measurement system comprises the sensing device and the circuit. These are shown in Figs. 2 and 3, respectively.

**1) Sensing Device:** To detect the deformation of the wrist shape corresponding to a finger motion, a sensing device was mounted on the user's wrist. The device can detect a deformation of the wrist shape from changes in the electrical contact resistance at the contact area between the skin of the wrist and the electrodes of the device. The device was curved to fit the wrist shape measured from one subject. Muscular contraction and movement of the tendons causes finger motion and a deformation of the wrist shape that corresponds to the variation in the sectional area of the muscles and tendons under the sensing device. As shown in Fig. 2, multiple grooves arranged on the skin side of the sensing device were fitted with electrodes  $D_{ci}$  ( $i = 1, 2, \dots, 16$ ). An earth electrode  $D_{ce}$  was also attached to the sensing device. When a finger moves, the flexible skin of the wrist deforms, covering the grooves in the sensing device and changing the contact area between the skin of the wrist and the sensing device. Because the contact area is inversely proportional to the electrical contact resistance, the electrical contact resistance changes as the skin of the wrist deforms.

**2) Measurement Circuit:** The measurement circuit detected the variation in the electrical contact resistance corresponding to a finger motion. The electrical contact resistance is related to the contact area, the conductivity of the material, the shape of object, the temperature, the condition of the skin surface, and other factors [24], [25]. In this research, we focused on variations in the electrical contact resistance influenced by the variations in the contact area for the use of short term. The skin electrode electrical contact resistance

is in the range of several hundred  $\text{k}\Omega \cdot \text{mm}^2$  to several hundred  $\text{M}\Omega \cdot \text{mm}^2$  and is influenced by the frequency of the applied voltage and the type of electrodes used [26]. In our system, the value of the electrical contact resistance was relatively large because the electrodes were made from conductive cloth. Fig. 3 shows the measurement circuit that outputs the voltage corresponding to the electrical contact resistance of each electrode.  $D_{ci}$  represents a sensing electrode. The electrical contact resistances of the sensing electrodes and the earth electrode are represented as  $R_{ci}$  ( $i = 1, 2, \dots, 16$ ) and  $R_{ce}$ , respectively. The circuit applied a DC voltage  $V_{in}$  to the skin through each electrode to cancel the skin and skin electrode capacitances that would otherwise complicate the detection of variation in electrical contact resistance.  $C_{\text{skin}}$ ,  $R_{\text{skin}}$ ,  $R_{\text{ref}}$ , and  $\alpha$  are the skin capacitance, skin resistance, reference resistance, and the gain of the instrumentation amplifier, respectively. As a dc voltage was used, we can regard only the skin resistance  $R_{\text{skin}}$  as the skin impedance. This skin resistance  $R_{\text{skin}}$  is less than approximately  $100 \text{ M}\Omega \cdot \text{mm}^2$  [27]. In this circuit,  $C_{\text{skin}}$ ,  $R_{\text{skin}}$ ,  $R_{\text{ref}}$ , and  $R_{ce}$  are constants. As the circuit represents internal body parts, the sensing electrodes were switched in time division by the multiplexer to detect variations in the electrical contact resistance of each electrode. The output voltages of each sensing electrode were expressed as  $V_{outi}$  ( $i = 1, 2, \dots, 16$ ), constituting an sixteen-dimensional vector  $\mathbf{v}$ .

### C. Multiple Regression Model

There are a number of ways of estimating finger joint angles from the system output. The complexity of the relationship between finger motion and the system output makes it extremely difficult to represent using an analytical method. In this study, a multiple regression model was adopted as a simple estimation method. The relationship between the joint angles of the finger allows the angle of an arbitrary joint to be estimated from the other joint angles [28], [29]. We defined the total finger joint angle as the sum of the joint angles for each finger, which reduced the 14 degrees of freedom of finger motion to 5 degrees of freedom corresponding to each finger. The estimated total finger joint angles for each finger constitute a five-dimensional vector  $\hat{\theta}$ . The multiple regression model was as follows:

$$\hat{\theta} = \mathbf{K}\phi(\mathbf{v}) \quad (1)$$

where  $\phi(\mathbf{v})$  is an  $M$ -dimensional basis function vector consisting of  $M - 1$  types of basis functions, e.g., a polynomial basis function, of output voltages  $\mathbf{v}$  and the bias element 1.  $\mathbf{K}$  is a  $5 \times M$  coefficient matrix that represents the relationship between the output voltage and the total finger joint angle. The parameters of the multiple regression model were calculated in advance and used to estimate the finger joint angles. Although the parameters are frequency dependent because of delays in the movement of muscles and tendons, the velocity of finger motion, and the capacitance of the skin and skin electrode, our simple multiple regression model disregarded frequency dependence. The deformation of the wrist shape corresponding to finger motion is different for the flexor and

extensor muscle types. For example, when the fingers flex, the flexor muscles contract and the palm side of the wrist becomes hollow. When the contact area between the skin and electrode decreases to reflect this hollowing, both the electrical contact resistance and the output voltage increase. The relationship between the finger joint angle and the output voltage is represented as a nonlinear equation that varies monotonically. Two types of multiple regression models were therefore used, with a first- and second-order polynomial basis function.

#### D. Calibration

The parameters of the multiple regression model  $\mathbf{K}$  were calculated using LSM. Synchronized real time series data from total finger joint angles and output voltages were recorded and used in LSM to calculate the parameters of the multiple regression models. The mean values of the output voltages in the section of each electrode were then calculated. The mean values of output voltages for each sensing electrode during one cycle of scanning were regarded as having been collected at the same time. The total finger joint angle of each finger was simultaneously measured by other sensing devices, e.g., a data glove. Then, the total finger joint angles at the mean time of each section for each electrode were calculated using linear interpolation. The mean value of each total finger joint angle in one cycle using all the sensing electrodes was then calculated and used with the mean values of the output voltages to calculate the parameters of the multiple regression models using LSM. The total finger joint angle of each finger was measured by another sensing device that was calibrated in advance, and constituted a five-dimensional vector  $\boldsymbol{\theta}$ . Then,  $T$  sets of time series data of actual total finger joint angles  $\boldsymbol{\theta}$  constituted a  $5 \times T$  matrix  $\Theta$ . Furthermore,  $T$  sets of time series data of output voltages  $\mathbf{v}_t$  ( $t = 1, 2, \dots, T$ ) were used to calculate the element values of  $M$ -dimensional basis functions  $\phi(\mathbf{v}_t)$ , and these basis functions constituted an  $M \times T$  matrix  $\Phi$ . The parameters of the multiple regression model  $\mathbf{K}$  were calculated from the matrices of actual total finger joint angles and basis functions using LSM, as follows:

$$\mathbf{K} \simeq \Theta \Phi^T \left( \Phi \Phi^T + \lambda \mathbf{I} \right)^{-1} \quad (2)$$

where  $\lambda \mathbf{I}$  is a regularization term and  $\lambda$  is a weight coefficient. The regularization term inhibits overfitting caused by the complexity of the regression model and the influence of outliers. The value of the weight coefficient of the regularization term that most effectively reduced the error of the estimated total finger joint angles was used in the evaluations. It was assumed that finger motion at low speed with high reproducibility could be used to derive parameters of the multiple regression model that are capable of accurately estimating the finger joint angles.

### III. EXPERIMENT

To investigate the practicality of the proposed system, we evaluated the accuracy of estimation of total finger joint angles, the adequacy of the multiple regression models, and the resolution of the estimation of total finger joint angles. We used a finger joint estimation system based on EMG

signals as a comparator. The joint angles of each finger and the output voltage or EMG signals from the forearm during flexion/extension were measured across several subjects, and the results were used to calculate the parameters of the multiple regression models and as metrics for evaluation. Finally, we visualized the finger motion using the estimated total finger joint angles.

#### A. Experimental Setup

We fabricated a sensing device and measurement circuit. The sensing device and the electrodes were produced from polylactic acid (PLA) and conductive cloth, respectively. The length of the major axis, minor axis, and the depth of a groove of the sensing device were 80, 60, and 2 mm, respectively. As PLA has a high Young's modulus of several GPa, the sensing device was not deformed by changes in the wrist shape. The number of electrodes was set at 16, and each electrode was arranged on a curved groove. The size of each rectangular electrode was  $20 \times 10$  mm. To stabilize the value of the output voltage, the switching period of the sensing electrodes should be larger than the rise time of the output voltage. The switching frequency was set at 60 Hz, i.e., a switching period of 0.017 s, as the rise time of the output voltage was 0.016 s. The gain  $\alpha$  of the instrumentation amplifier was set at 10. We used a 5 V battery as the DC source and an AD/DA module (National Instruments, NI USB-6216) to record the output voltage and control the multiplexer. The output voltage was recorded at a sampling rate of 1 kHz and a quantifying bit number of 16 bits. EMG signals of eight channels from the forearm were recorded by a gesture control armband (Thalmic Labs, Myo) [14] with a sampling rate of 1 kHz and a quantifying bit number of 8 bits. The finger joint angles were recorded by a data glove (5DT, Data Glove 14 Ultra) with a sampling rate of 60 Hz and a quantifying bit number of 12 bits. The data glove was capable of measuring the angles of the IP and MP joints of the thumb, and the angles of the PIP and MP joints of the fingers. The angles of the DIP joints can be estimated from the angles of the PIP joints owing to the relationship between them [30]. The start time of the sampling for each device was synchronized by a starting trigger from the command line input.

#### B. Procedure

Nine male subjects aged between 22 and 30 participated in the experiment after giving informed consent. For the evaluation of the proposed system, the subjects mounted the data glove on their right hand and the fabricated sensing device on their right wrist. Because the hand circumference is different between the subjects, the mounting position of the sensing device was adjusted to fit the curvature of the device to the wrist shape of individual subject. The sensing device was mounted so that electrodes  $D_{c8}$  and  $D_{c9}$  were fixed on the wrist skin of the thumb, and  $D_{c1}$  and  $D_{c16}$  on that of the little finger. For the evaluation of the EMG system, the subjects mounted the data glove and the EMG device on their right hand and forearm, respectively. No skin preparation, such as shaving, cleaning, or moisturizing was used. As shown in Fig. 4, each subject sat in a chair and maintained the

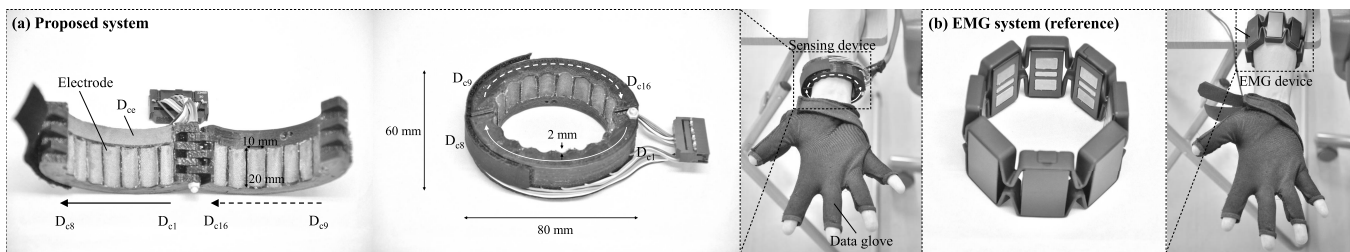


**Fig. 4.** Experimental setup. (a) Proposed system: a data glove and the fabricated sensing device were mounted on a subject's right hand and wrist, respectively. (b) EMG system: a data glove and EMG device were mounted on a subject's right hand and forearm. The subjects maintained the posture of their wrist, elbow, and forearm.

posture of the wrist, elbow, and forearm in order to control the experimental conditions. To mimic a grasping action, each subject was asked to flex and extend all five fingers to the maximum joint angle at 4 s intervals, following a metronome. The trial was repeated three times (one familiarization and two evaluation trials) for the proposed and EMG systems by all subjects. In each trial, 400 sets of output voltages from all sensing electrodes or EMG signals and finger joint angles were recorded. The experiment was approved by the Ethical Committee of the Graduate School of Engineering Science (26-4), Osaka University, Japan.

### C. Metrics

Evaluations were conducted using two types of multiple regression model comprising a first- and second-order polynomial basis function to compare the experimental results and investigate the influence of the order of the polynomial basis function. For regularization, the value of the weight coefficient  $\lambda$  of the regularization term for each multiple regression model must be determined. The root-mean-square error (RMSE) of the estimated total finger joint angles was calculated using the total finger joint angles of the evaluation data for each finger, subject, and trial. The value of the weight coefficient that minimized the mean RMSE value for all fingers, subjects, and trials was derived. First, RMSEs with a weight coefficient varying at intervals of 25 in the range  $-500$  to  $2500$  were calculated. This range was selected based on the approximate shape of the weight coefficient-RMSE profile. Then, RMSEs with a weight coefficient varying at intervals of 0.1 in the range of minimal solutions  $\pm 25$  were calculated in order to determine the optimal value of the weight coefficient more precisely. Finally, the value of the weight coefficient that minimized the mean value of RMSE for all fingers, subjects, and trials was determined and used as the optimal solution.

In this experiment, three metrics were used to evaluate the estimation of finger joint angles by the proposed system and the EMG system. The first metric was the accuracy of estimation of the total finger joint angles. The RMSE of the estimated total finger joint angles was used to represent the magnitude of error between the actual and estimated finger joint angles. The second metric was the adequacy of the multiple regression models, represented by the coefficient of determination ( $R^2$ ), which represents the suitability of data fitting to a multiple regression model. The third metric was the resolution of the estimation of the total finger joint angles, represented as the

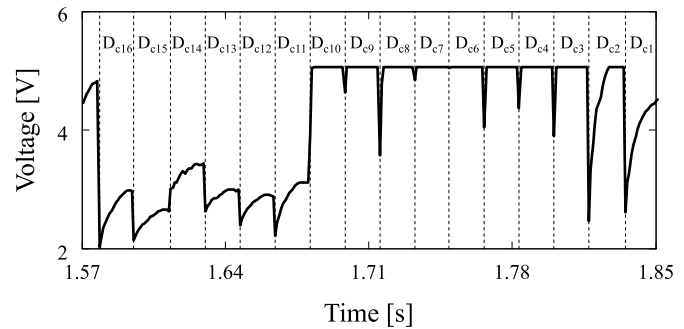


**Fig. 5.** Example of output voltage of the system in time series. The output voltages of each sensing electrode were recorded in a time division.

standard deviation (SD) of distances between the estimated and actual total finger joint angles. This represented the ability to detect variations in the estimated finger joint angles. To estimate finger angles from the EMG signals, the signals were rectified, low-pass filtered (5 Hz cut-off frequency, moving average of 80 sample points), and used for multiple regression analysis, in the same way as those from the proposed system. The first 200 sets of recorded data were used to calculate the parameters of the multiple regression models (calibration data), whereas the second 200 sets were used to calculate the metrics (evaluation data).

### D. Results

**Fig. 5** shows a representative example of the output voltages in a time series measured using all sensing electrodes in one cycle. These were taken from one trial by one subject. The proposed system was able to measure the different values of the output voltages from each sensing electrode. The results showed that the transient period after the DC voltage was applied to the electrode was longer than the switching period between consecutive electrodes. Although we assumed quasi DC measurement, the output voltage will be influenced by the capacitive elements in the skin. However, as shown in **Fig. 6**, the output voltage varied according to the contact state. **Fig. 6** shows the output voltages from the proposed system subdivided into sections for each sensing electrode, the rectified and smoothed EMG signals, and the total finger joint angles of the middle finger of one subject. As shown in **Fig. 6(a)**, it was confirmed that the output voltages of each electrode varied in line with the variation of the total finger

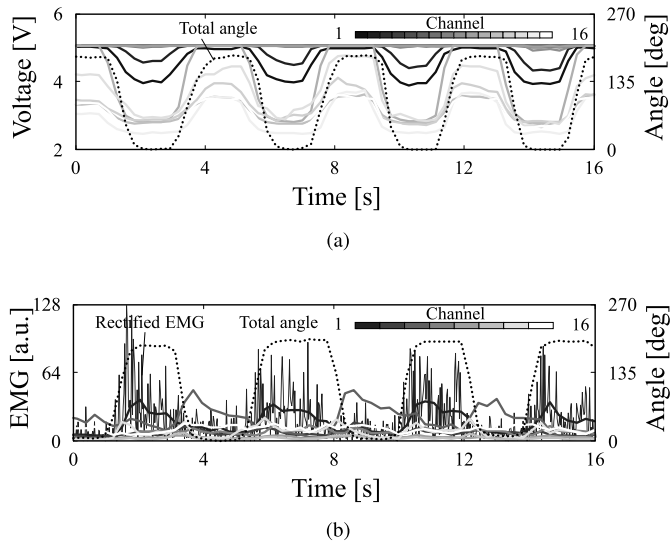


**Fig. 6.** Example of the total finger joint angle of the middle finger. (a) Output voltages of each electrode in a time series; (b) rectified and smoothed EMG signals. The total finger joint angle is shown by a black dashed line and the output voltages and EMG signals are shown by gray scale solid lines.

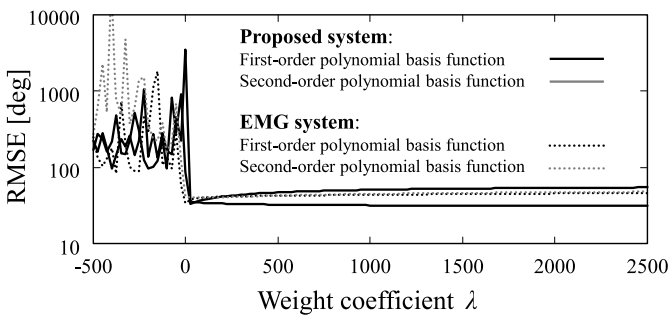


**Fig. 7.** RMSEs calculated at different values of weight coefficient. RMSEs of multiple regression models with a first- and second-order polynomial basis function are shown by black and gray lines, respectively. RMSEs of the proposed and EMG systems are shown by solid and dashed lines, respectively.

joint angle. The magnitude of variation in the output voltage was different for different electrodes. The parameters of the multiple regression model were then calculated from these calibration data using LSM.

**1) Determination of the Regularization Term:** Fig. 7 shows the mean RMSE values of the proposed and EMG systems at different values of the weighting coefficient using the two multiple regression models. We found that the weight coefficients of the minimum RMSEs under the two models were  $\lambda = 9.8$  and  $\lambda = 2440.3$  (proposed system), and  $\lambda = 0.8$  and  $\lambda = 101.2$  (EMG system), respectively. These four values of weighting coefficient were used in the following evaluations. Comparison of the RMSE values from the two types of multiple regression model confirmed that the optimal value of the weight coefficient depended on the order of the multiple regression model used.

**2) Accuracy of Estimation:** Fig. 8 shows a representative estimation result using the proposed system for total finger joint angles with evaluation data taken from one trial by one

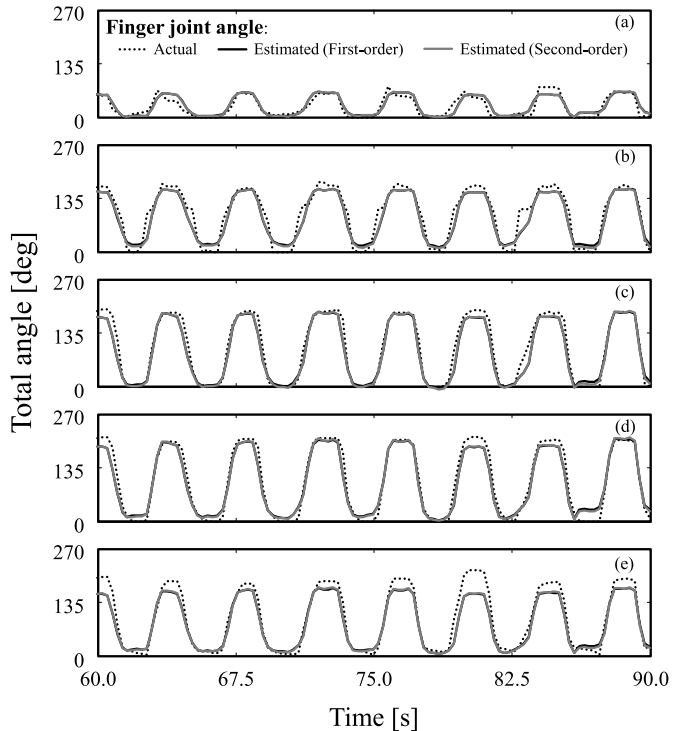


**Fig. 8.** Estimation results of the total finger joint angles using the proposed system with evaluation data. (a) Thumb. (b) Index finger. (c) Middle finger. (d) Ring finger. (e) Little finger. Actual and estimated total finger joint angles with a first- and second-order polynomial basis function are shown by black dashed line, and black and gray solid lines, respectively.

subject. The estimated total finger joint angle was shown to be in good agreement with the actual total finger joint angle. It was also confirmed that the error increased as the degree of bending of the finger increased. Table I shows the mean values and standard deviations of the RMSEs for each finger, for all subjects and trials. The estimated mean RMSE values were 29–34 degrees for the proposed system and 32–44 degrees for the EMG system. In comparison with the maximum values of total finger joint angles, which were 180 degree for the thumb and 270 degree for the other finger, the mean RMSE values were small. The large standard deviations confirmed that there were differences in accuracy between individual subjects.

**3) Adequacy of Multiple Regression Models:** The coefficient of determination ( $R^2$ ) for each multiple regression model was calculated for all subjects, trials, and fingers. The mean values and standard deviations of the coefficient of determination are shown in Table I. For the proposed system, it was confirmed that the coefficients of determination when using a second-order polynomial basis function were larger than those of the first-order polynomial basis function for the index, middle, ring, and little fingers. A multiple regression model with a second-order polynomial basis function was shown to be suitable for estimating the total finger joint angles of these fingers.

**4) Resolution of Estimation:** The variances in absolute values of differences between the estimated and actual total finger joint angles were calculated for all subjects, trials, and fingers. SD, which represents the resolution of the estimation of the total finger joint angles, was then calculated from

**TABLE I**  
METRICS (RMSE, R<sup>2</sup>, AND SD) FOR THE PROPOSED AND EMG SYSTEMS WITH TWO TYPES OF REGRESSION MODEL

| System                 | Metrics      | Model order | Thumb          | Index finger | Middle finger | Ring finger | Little finger |
|------------------------|--------------|-------------|----------------|--------------|---------------|-------------|---------------|
| <b>Proposed system</b> | RMSE [deg]   | first       | 29.0±9.93      | 34.3±10.2    | 32.5±11.1     | 32.2±9.82   | 33.2±10.3     |
|                        |              | second      | 29.1±10.3      | 34.0±10.7    | 30.9±9.33     | 31.0±9.75   | 32.7±10.4     |
|                        | $R^2$ [a.u.] | first       | 0.0504±0.524   | 0.660±0.178  | 0.809±0.155   | 0.797±0.137 | 0.375±0.461   |
|                        |              | second      | 0.0358±0.563   | 0.662±0.199  | 0.831±0.109   | 0.812±0.124 | 0.386±0.466   |
|                        | SD [deg]     | first       | 16.5±5.52      | 18.8±5.48    | 18.8±6.89     | 17.9±5.47   | 19.4±5.45     |
|                        |              | second      | 16.7±5.71      | 18.4±5.42    | 18.0±5.10     | 17.4±5.16   | 19.2±5.36     |
| <b>EMG system</b>      | RMSE [deg]   | first       | 31.6±9.42      | 31.5±8.84    | 36.2±8.73     | 35.8±8.32   | 34.6±9.84     |
|                        |              | second      | 39.2±16.7      | 40.8±11.8    | 40.5±12.0     | 39.3±10.8   | 44.1±23.6     |
|                        | $R^2$ [a.u.] | first       | -0.00858±0.997 | 0.728±0.117  | 0.770±0.136   | 0.767±0.138 | 0.534±0.270   |
|                        |              | second      | -0.950±2.58    | 0.547±0.190  | 0.699±0.216   | 0.706±0.222 | 0.0252±1.04   |
|                        | SD [deg]     | first       | 18.8±5.60      | 19.8±6.24    | 22.1±6.36     | 22.0±7.00   | 21.1±6.57     |
|                        |              | second      | 26.4±14.8      | 28.4±9.59    | 27.4±10.0     | 26.5±9.13   | 31.8±21.7     |

these variances. **Table I** shows the mean values and standard deviations of SD for the proposed and EMG systems for all subjects, trials, and fingers. The results demonstrated that the total finger joint angles could be estimated with a resolution of approximately 17–19 degrees by the proposed system and 19–32 degrees by the EMG system. A one-tailed paired sample t-test between the SDs of the two systems for the two types of regression model showed a significant difference ( $p < 0.01$ ). For the proposed system, the minimum and maximum SDs for all subjects and trials were 6.36 and 41.8 degrees for the multiple regression model with a first-order polynomial basis function, and 6.27 and 31.6 degrees for a multiple regression model with a second-order polynomial basis function.

### E. Visualization

To intuitively confirm the estimation results and demonstrate a practical application to biomechanics and human-computer interactions, the estimated total finger joint angles were visualized in real-time. The distal, proximal, and metacarpal phalanges of the thumb and the distal, middle, proximal, and metacarpal phalanges of the fingers were visualized to demonstrate the finger motion. The angles of the carpometacarpal (CMC) joint were fixed at 0 degrees. The angles of the IP and MP joints of the thumb and the DIP, PIP, and MP joints of the fingers were determined using the estimated total finger joint angles and based on the relationship between the joint angles of a finger [28], [29]. A first-order polynomial basis function was used to estimate the finger joint angles. In this experiment, one subject was asked to flex and extend a finger to provide calibration data. The finger motions of flexion, extension, and grasping were then visualized. During calibration and visualization, the postures of the wrist, elbow, and forearm were fixed as shown in **Fig. 9(a)**. A table tennis ball and a baseball were used as grasped objects to demonstrate the robustness of the proposed system. **Fig. 9** shows a representative example of the visualized finger motion. It was confirmed that the estimated flexion and extension finger motions were similar to the actual motions. As shown in **Fig. 9(b)**, the system demonstrated robust estimation of the finger joint angles when the user grasped an object. Furthermore, **Fig. 9(c)** shows that the proposed system was also able to approximate the finger joint angles when the postures of the wrist, elbow, and forearm were different from

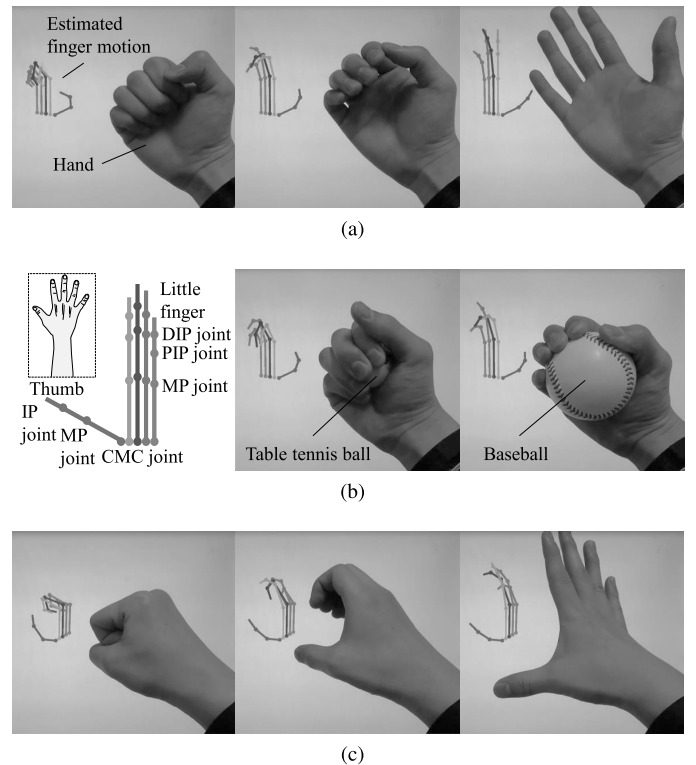


**Fig. 9.** Visualized finger motion. Each finger joint angle was determined based on the estimation. (a) Flexion and extension of five fingers with the postures of the wrist, elbow, and forearm the same as those used during calibration. (b) Grasping objects. (c) Flexion and extension of five fingers with postures of the wrist, elbow, and forearm different from those used during calibration.

those used for calibration. However, it became difficult to derive the complex finger motion owing to the low measurement resolution of the deformation of the wrist shape. As the switching period of the sensing electrodes was set at 0.017 s, 0.272 s per cycle was required to involve all the electrodes. However, the system was shown to be capable of estimating finger joint angles at a frequency of 3.676 Hz, which exceeds most normal hand actions.

## IV. DISCUSSION

### A. Feasibility

The proposed system was able to estimate total finger joint angles with mean RMSE values of 29–34 degrees and a

resolution of approximately 17–19 degrees. By dividing these values by the number of joints of each finger, we can conclude that the angle of each finger joint can be estimated with mean RMSE values of 10–15 degrees and a resolution of approximately 6–8 degrees. The resolution of the proposed system was significantly better than that of the EMG system. This may be due to a superior signal to noise ratio, as the signal in the proposed system has a level of several volts, whereas the EMG system amplifies a signal in the millivolt range. As shown in Fig. 8, there is a larger difference between actual and estimated total finger joint angles at large joint angles. A possible explanation is that the grasping force by the subject during data sampling is not constant. Fig. 9(c) shows that the proposed system was able to approximate the finger joint angles even when the forearm was pronated. Although these RMSEs and resolutions are not fine enough for applications requiring highly accurate tracking of finger motion, they are sufficient for use in applications such as system inputs.

### B. Model and Calibration

As shown in Table I, the coefficients of determination of the multiple regression model were larger than 0.8 for the middle and ring fingers. This confirmed that the multiple regression models used in our experiment was suitable for use in the estimation of the total finger joint angles of these fingers, where the simplicity of motion during flexion and extension seems to produce a linearity between the finger joint angle and the output voltage. However, these multiple regression models were not suitable for highly accurate estimation of the joint angles of the thumb. Since the CMC joint of the thumb has more degrees of freedom than that of the other fingers, thumb motion differs between subjects, making the recorded finger joint angles used for calculating the parameters of the multiple regression models more complex. The relationships between fingers and between the joint angles of a finger were not used in our experiments, and it is possible that these may allow the estimation of complex finger motion. Owing to the complexity of hand motion, better calibration processes will need to be developed for future applications. In this experiment, subjects were asked to flex and extend the finger within 4 s, to allow data to be recorded while the finger was moving. This low speed of the finger motion enabled detailed variations of the finger joint angles to be recorded and was effective for calibration. To estimate more complex finger motion, data recorded with various finger motions, e.g., flexion/extension of each finger, will be needed. Measurement errors when using the data glove, and the low reproducibility of finger motion, also affected the calibration results.

### C. Limitations

Complex finger motion also increases the complexity of the associated muscle and tendon activity. This creates a further challenge, as detecting the deformation of the wrist shape becomes more difficult. To capture more complex finger motion, the independence of each sensing electrode should be improved to reduce the influence of a single electrode on the behavior of the overall system. For example, a sigmoid basis

function may be effective. Increasing the number of electrodes and optimizing the structure of the sensing device and the arrangement of electrodes may also be effective ways of achieving more accurate detection of deformations of the wrist. The number of electrodes could be increased by modifying the size, and sensitivity of the electrodes or switching the frequency of the sensing electrodes.

To estimate faster finger motion, the sampling frequency and switching frequency of the sensing electrodes must be considered owing to the switching of electrodes in time division. Kuboyama et al. reported an upper limit to the frequency of finger flexion/extension at approximately 8 Hz [31]. To allow estimation of finger motion greater than 8 Hz, the switching frequency should be above 128 Hz. In contrast, the switching frequency of the proposed system was set at 60 Hz. To overcome this, the rise time of the voltage output should be modified to improve the switching speed. Because the output voltage increases exponentially with respect to time, the output voltage varies in line with the contact resistance, even if the switching speed is increased. However, a higher switching frequency reduces the sensitivity of the system. The frequency division method may offer an alternative solution to this problem.

It can be assumed that the contact area will vary slightly owing to deformation of the wrist shape caused by pronation/supination of the forearm and the weight of the sensing device. Such variation in the contact area will reduce the accuracy with which the finger joint angles can be estimated. In our experiments, the postures of the wrist, elbow, and forearm were fixed to prevent their motion influencing the deformation of the wrist. To achieve robust measurements that are not dependent on the environment or the type of action being performed, the influence of wrist, elbow, and forearm motion should be considered. For example, we should consider the effect of pronation/supination of the forearm. A previous study using infrared photo reflectors to measure the wrist shape showed that recognition of hand posture was possible even when the forearm was pronated and supinated [16]. This suggests that our own system will also be able to deal with the influence of the pronation/supination of the forearm. In addition, our sensing device is stable on the user's wrist and little influenced by gravity, as it uses thin and light electrodes. As the sensing device has approximately the same weight as a wristwatch, at 0.067 kg, it is small enough for use in daily life. Furthermore, it does not need to press strongly on the wrist, as it relies only on contact between the skin and electrodes. This should make wearing the device acceptable to users.

An outstanding problem with the proposed method is that the electrical contact resistance is altered by the condition of the skin, such as the amount of sweat present. Furthermore, aging effects and individual differences in skin type and wrist structure influence the electrical contact resistance and the parameters of the multiple regression model, respectively. The use of a reference electrode to normalize the output voltage can compensate for these. Because the performance of the system depends on the skin electrode contact, the sensing device needs to be fixed firmly to ensure high reproducibility.

## V. CONCLUSION

We proposed a novel finger motion capture method based on electrical contact resistance measured at the wrist. A sensing device with 16 electrodes outputs a voltage corresponding to the electrical contact resistance, and this was used to detect the deformation of the wrist when a finger was moved. Multiple regression models were constructed, with parameters calculated from measured system output voltages and total finger joint angles using LSM. Finger joint angles were then estimated using these models and the output voltage. We experimentally investigated the accuracy of finger joint angle estimation, the adequacy of two types of multiple regression model, and the resolution of the total finger joint angle estimation. The mean RMSE values of the estimated total finger joint angles were approximately 29–34 degrees. The multiple regression model with a second-order polynomial basis function was found to be well suited to the estimation of all total finger joint angles, but not those of thumb. We conclude that the proposed method is able to estimate finger motion within a reasonable degree of accuracy, while placing fewer restrictions on the environment in which it can be used and on the actions of the user. Although further improvement is required, the proposed system is a potentially useful tool for ubiquitous finger motion capture.

## REFERENCES

- [1] J. K. Aggarwal and Q. Cai, "Human motion analysis: A review," *Comput. Vis. Image Understand.*, vol. 73, no. 3, pp. 428–440, Mar. 1999.
- [2] H. Zhou and H. Hu, "Human motion tracking for rehabilitation—A survey," *Biomed. Signal Process. Control*, vol. 3, no. 1, pp. 1–18, 2008.
- [3] A. Erol, G. Bebis, M. Nicolescu, R. D. Boyle, and X. Twombly, "Vision-based hand pose estimation: A review," *Comput. Vis. Image Understand.*, vol. 108, nos. 1–2, pp. 52–73, Oct./Nov. 2007.
- [4] R. Y. Wang and J. Popovic, "Real-time hand-tracking with a color glove," *ACM Trans. Graph.*, vol. 28, no. 3, pp. 63:1–63:8, 2009.
- [5] L. Motion. (2016). *Leap Motion Controller*. [Online]. Available: <https://www.leapmotion.com/>
- [6] D. Kim *et al.*, "Digits: Freehand 3D interactions anywhere using a wrist-worn gloveless sensor," in *Proc. 25th Annu. ACM Symp. User Interface Softw. Technol.*, 2012, pp. 167–176.
- [7] D. J. Sturman and D. Zeltzer, "A survey of glove-based input," *IEEE Comput. Graph. Appl.*, vol. 14, no. 1, pp. 30–39, Jan. 1994.
- [8] T. G. Zimmerman, J. Lanier, C. Blanchard, S. Bryson, and Y. Harvill, "A hand gesture interface device," *ACM SIGCHI Bull.*, vol. 18, no. 4, pp. 189–192, 1987.
- [9] M. M. Rahman, K. Mitobe, M. Suzuki, C. Takano, and N. Yoshimura, "Analysis of dexterous finger movement for piano education using motion capture system," *Int. J. Sci. Technol. Edu. Res.*, vol. 2, no. 2, pp. 22–31, 2011.
- [10] L. Dipietro, A. M. Sabatini, and P. Dario, "A survey of glove-based systems and their applications," *IEEE Trans. Syst., Man, Cybern. C, Appl. Rev.*, vol. 38, no. 4, pp. 461–482, Jul. 2008.
- [11] M. Yamada, N. Niwa, and A. Uchiyama, "Evaluation of a multifunctional hand prosthesis system using emg controlled animation," *IEEE Trans. Biomed. Eng.*, vol. 30, no. 11, pp. 759–763, Dec. 1983.
- [12] J. G. Ngeo, T. Tamei, and T. Shibata, "Continuous and simultaneous estimation of finger kinematics using inputs from an EMG-to-muscle activation model," *J. NeuroEng. Rehabil.*, vol. 11, no. 122, pp. 1–14, 2014.
- [13] F. V. G. Tenore, A. Ramos, A. Fahmy, S. Acharya, R. Etienne-Cummings, and N. V. Thakor, "Decoding of individuated finger movements using surface electromyography," *IEEE Trans. Biomed. Eng.*, vol. 56, no. 5, pp. 1427–1434, May 2009.
- [14] Thalmic Labs Inc. (Mar. 9, 2016). *Myo*. [Online]. Available: <https://www.myo.com/>
- [15] R. Fukui, M. Watanabe, M. Shimosaka, and T. Sato, "Development of wrist contour measuring device for an interface using hand shape recognition," *Adv. Robot.*, vol. 27, no. 7, pp. 481–492, 2013.
- [16] R. Fukui, M. Watanabe, M. Shimosaka, and T. Sato, "Hand shape classification in various pronation angles using a wearable wrist contour sensor," *Adv. Robot.*, vol. 29, no. 1, pp. 3–11, 2015.
- [17] J. Rekimoto, "GestureWrist and GesturePad: Unobtrusive wearable interaction devices," in *Proc. IEEE 5th Int. Symp. Wearable Comput.*, Oct. 2001, pp. 21–27.
- [18] A. Dementev and J. A. Paradiso, "WristFlex: Low-power gesture input with wrist-worn pressure sensors," in *Proc. 27th Annu. ACM Symp. User Interface Softw. Technol.*, 2014, pp. 161–166.
- [19] T. Deyle, S. Palinko, E. S. Poole, and T. Starner, "Hambone: A bio-acoustic gesture interface," in *Proc. 11th IEEE Int. Symp. Wearable Comput.*, Oct. 2007, pp. 3–10.
- [20] B. Amento, W. Hill, and L. Terpening, "The sound of one hand: A wrist-mounted bio-acoustic fingertip gesture interface," in *Proc. Extended Abstracts Human Factors Comput. Syst.*, 2002, pp. 724–725.
- [21] S. Sikdar *et al.*, "Novel method for predicting dexterous individual finger movements by imaging muscle activity using a wearable ultrasonic system," *IEEE Trans. Neural Syst. Rehabil. Eng.*, vol. 22, no. 1, pp. 69–76, Jan. 2014.
- [22] J. Lin *et al.*, "BackHand: Sensing hand gestures via back of the hand," in *Proc. 28th Annu. ACM Symp. User Interface Softw. Technol.*, 2015, pp. 557–564.
- [23] L. A. Jones and S. J. Lederman, *Human Hand Function*. Oxford, U.K.: Oxford Univ. Press, 2006.
- [24] G. Windred, "Electrical contact resistance," *J. Franklin Inst.*, vol. 231, no. 6, pp. 547–585, 1941.
- [25] R. Holm, *Electric Contacts: Theory Application*. Berlin, Germany: Springer, 2013.
- [26] M. S. Spach, R. C. Barr, J. W. Havstad, and E. C. Long, "Skin-electrode impedance and its effect on recording cardiac potentials," *Circulation*, vol. 34, no. 4, pp. 649–656, 1966.
- [27] H. Antoni, A. Chilbert, and D. Sweeney, *Applied Bioelectricity From Electrical Stimulation to Electropathology*, J. P. Reilly, Ed. New York, NY, USA: Springer, 1998.
- [28] H. Rijpkema and M. Girard, "Computer animation of knowledge-based human grasping," *ACM SIGGRAPH Comput. Graph.*, vol. 25, no. 4, pp. 339–348, 1991.
- [29] V. I. Pavlovic, R. Sharma, and T. S. Huang, "Visual interpretation of hand gestures for human-computer interaction: A review," *IEEE Trans. Pattern Anal. Mach. Intell.*, vol. 19, no. 7, pp. 677–695, Jul. 1997.
- [30] J. W. Lee and K. Rim, "Maximum finger force prediction using a planar simulation of the middle finger," *J. Eng. Med.*, vol. 204, no. 3, pp. 169–178, 1990.
- [31] N. Kuboyama, T. Nabetani, K. Shibuya, K. Machida, and T. Ogaki, "Relationship between cerebral activity and movement frequency of maximal finger tapping," *J. Phys. Anthropol. Appl. Human Sci.*, vol. 24, no. 3, pp. 201–208, 2005.

**Junki Kawaguchi** received the M.S. degree in engineering from Osaka University, Osaka, Japan, in 2016.

He is presently with DENSO Corporation. His research interests include biomedical instrumentation.



**Shunsuke Yoshimoto** (M'13) received the Ph.D. degree in engineering from Osaka University, Osaka, Japan, in 2012.

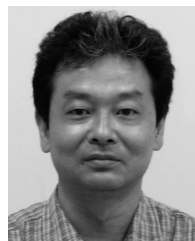
Since 2012, he is an Assistant Professor of Graduate School of Engineering Science at Osaka University. His research interests include haptic interaction technologies and biomedical instrumentation.





**Yoshihiro Kuroda** (M'14) received the Ph.D. degree in informatics from Kyoto University, Kyoto, Japan, in 2005.

He was an Assistant Professor of Graduate School of Engineering Science at Osaka University from 2006 to 2013 and he was an Associate Professor of Cybermedia Center at Osaka University from 2013 to 2016. From 2016, he is an Associate Professor of Graduate School of Engineering Science at Osaka University. His research interests include haptic interaction technologies and biomedical engineering.



**Osamu Oshiro** (M'00) received the Ph.D. degree in engineering from Osaka University, Osaka, Japan, in 1990.

He was a research engineer of Sumitomo Metal Industries from 1990 to 1993 and he was an Assistant/Associate Professor of Nara Institute of Science and Technology from 1993 to 2003. From 2003, he has been a Professor of Graduate School of Engineering Science, Osaka University. His research interests focus PBR, fac-

ing technology, modeling of distributed human

system, and so on.